Chapter 5

Grain Boundary Segregation in Nanocrystructured Metallic Materials

Jinyu Zhang, Gang Liu and Jun Sun

Additional information is available at the end of the chapter

http://dx.doi.org/10.5772/66598

Abstract

The aim of this chapter is to shed light on the effects of grain boundary segregation on microstructural evolution in nanostructured metallic materials as well as on their mechanical properties. Several key topics will be covered. First, a brief explanation of mechanical stress-driven grain growth in nanostructured Al, Ni, and Cu thin films will be provided in terms of a deformation mechanism map. It will become clear that the excess energy of grain boundaries enable the nanostructured metals to suffer from significant microstructure evolution via dislocation-boundary interactions during plastic deformation even at room temperature. Manipulation of grain boundary structures/properties via dopants segregation at grain boundaries to inhibit grain coalescence associated with remarkably enhanced mechanical properties is then discussed in three representative binary Cu-based systems, i.e., Cu-Zr, Cu-Al, and Cu-W. This is finally followed by a summary of this chapter.

Keywords: nanostructured materials, mechanical properties, grain boundary segregation, grain growth, twinning

1. Introduction

The nanoscaled internal features, in which two quantities, i.e., the *characteristic length* and the *size parameter* likely overlap, render the conventional deformation mechanisms and size laws often break down and even be reversed in nanostructured (NS) metallic materials, including nanocrystalline (NC) and nanotwinned (NT) materials [1–3]. Indeed, for many purposes, making the crystals as small as possible provides significant advantages in performance, but such materials are often unstable: The crystals tend to merge and grow larger even at room temperature (RT) [4–7]. To suppress the nanograin growth and maintain the nanoscale microstructure, two approaches can be adopted [8–15]: (i) Thermodynamic approach: reduction

of the driving force for grain growth by segregation of the solutes at the grain-boundaries (GBs), (ii) Kinetic approach: reduction of the GB mobility, by e.g., porosity, solute atoms, and precipitates at the GBs, which impose drag forces.

In this chapter, first, a brief introduction of mechanical stress-driven grain growth in NS Cu and Ni thin films/foils as well as their mechanical properties will be provided in terms of size-dependent deformation mechanisms. Subsequently, dopants segregation at GBs to hinder grain coarsening and enhance mechanical properties via the alloying method is discussed in three representative binary Cu-based systems, i.e., Cu-Zr, Cu-Al, and Cu-W.

2. Synthesis, microstructural characterizationw and mechanical tests

The synthesis of NS metallic thin films can be achieved by several bottom-up techniques, such as physical vapor deposition (PVD) and electrodeposition (ED), in which the choice of deposition conditions has a tremendous influence on the microstructural features and mechanical properties of these NS metallic films/foils.

PVD is the most common approach to fabricate metallic thin films/foils, including evaporation, sputtering, and less commonly molecular beam epitaxy [16, 17]. Compared with other methods, magnetron sputtering (MS) can clean the substrate by "backsputtering" and generate greater impact angles of the sputtered atoms onto the substrate, resulting in smaller surface roughness of the film by covering the defects and/or step on the substrate [17]. Although, MS increases the possibility of crystal damage due to high impact energies of sputtered atoms, it is still the most widely used method to prepare thin films.

ED is a technique within the broader group of electrochemical synthesis methods and uses an electric current to deposit pure metals from an aqueous, electrolytic solution [18, 19]. Compared with PVD, ED offers a lower cost and faster low-temperature deposition method. It displays remarkable advantages to synthesize highly dense NC materials with (1) few size and shape limitations, (2) tunable microstructural size parameters, and (3) hierarchical structures, e.g., a bimodal grain size-distribution [20] and NT grains [21], providing potential benefits to mechanical performance. Especially, these nanotwins improve both the mechanical strength and ductility, yet maintain high electric conductivity [22].

The crystalline structure, orientation, and grain boundaries within metallic thin films could be experimentally probed by suitable techniques, including X-ray diffraction (XRD), scanning and transmission electron microscopy (SEM and TEM), combining with other more superior appurtenances, such as the electron backscattered diffraction (EBSD) system and the precession-enhanced electron diffraction (PED) system. The chemical conuration of the materials can be characterized by the energy dispersive X-ray (EDX) and the powerful 3-D atom probe tomography (APT).

Due to the difficulty in performing the mechanical tests on the free-standing metallic thin films often with thickness of roughly 1 μm or less, researchers put great emphasis on the substrate-supported thin films. For example, the tensile ductility and fatigue lifetime of metallic

thin films on flexible substrates, both of which are characterized by the critical strain to nucleate microcracks [23, 24], can be determined by a Micro-Force Test System (MTS® Tytron 250) at RT. By contrast, the strength/hardness and modulus of thin films on rigid substrates can be measured using instrumented nanoindenter apparatus (e.g., TI950 TriboIndenter, Nano XP) often equipped with a standard Berkovich tip and a diamond flat punch. In what follows, we will mainly concentrate on the mechanical properties of substrate-supported metallic (alloyed) NS thin films.

3. Microstructure-mechanical properties correlation of nanostructured pure FCC metals

This section is divided into three subsections. The subsection on size-dependent deformation mechanisms is introduced based on a deformation-mechanism map. Microstructural evolution, in particular, the steady-state grain size, is then discussed in terms of a dislocation-based mechanism. The mechanical properties subsection contrasts yield strength, ductility, strain-rate sensitivity, and fatigue lifetime in NS metals.

3.1. Size-dependent deformation mechanisms

In coarse-grained (CG) metals (grain size $d \geq 1$ μm), deformation of the material is believed to occur through the generation and motion of dislocations within the individual grains. As the grain size decreases, it is normally expected that with GBs now occupying a significant volume fraction of the material, deformation proceeds by a mechanism that is intergranular rather than intragranular in nature.

Yamakov and colleagues [25] constructed a deformation mechanism map in NC FCC metals using information obtained from molecular dynamics (MD) simulations (see **Figure 1**), revealing how the crossover with decreasing d from dislocation-driven to GB-mediated deformation depends on the stacking-fault energy (SFE, γ_{sf}), the elastic properties of the material, and the magnitude of the applied stress. This deformation map can be divided into three regions in light of the competition between the grain size d and the dislocation splitting distance r. Region I encompasses larger d and/or higher γ_{sf}, where plastic deformation is dominated by full (perhaps extended) dislocations that nucleate from GBs and propagate across grains. Region II involves smaller d and/or lower γ_{sf}, where partials nucleate and propagate across grains, associated with production of stacking-faults (SFs) that inhibit subsequent dislocation motion and induce strain hardening. Region III corresponds to the smallest d or lowest stress regime, where no dislocations are present and deformation is dominantly controlled by GB-mediated mechanism, resulting in an inverse H-P effect. Although these MD simulations performed at unrealistically large strain rates (10^7–10^9 s^{-1}), their findings agree well with the experiment observations about the transition from full dislocations to partials and finally to GB-mediated processes.

Where do dislocations in NC metals go if they are the dominant plastic carriers? Actually, in the MD simulations, a key deformation process is dislocation nucleation at a GB, glide across grain interiors that are free of obstacles, and are absorbed by the opposite GB [26, 27].

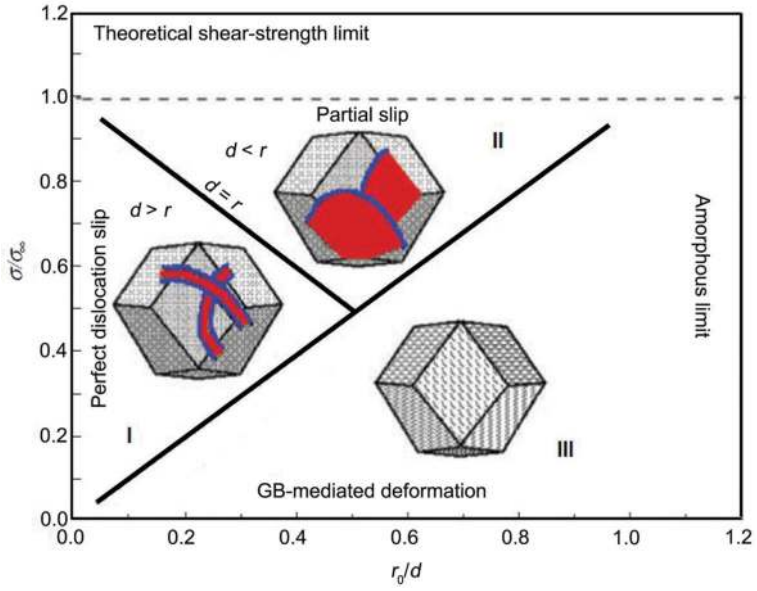

Figure 1. A deformation-mechanism map incorporating the role of the SEF for FCC NC metals at low temperature. The map shows three distinct regions in which either complete extended dislocations (Region I) or partial dislocations (Region II), or no dislocations at all (Region III) exist during the low-temperature deformation of FCC NC metals. The map is expressed in reduced units of stress (σ/σ_∞) and inverse grain size (r_0/d).The parameters σ_∞ and r_0 are functions of the SEF and the elastic properties of the material. Figure is taken with permission from Ref. [25].

Both *in situ* and *ex situ* experiments have unambiguously demonstrated that the reversible motion of dislocations emitted from GBs accompanied with weak storage even starvation of dislocations in grain interiors in deformed NC FCC metals, leaving behind deformation twins (terminated at GBs) and SFs in general at upper and lower nanoregime, respectively [28–34]. In this context, GBs act as dislocation sources as well as sinks.

In parallel, several theoretical models have been proposed to predict the crossover grain size (d_C) between emitted full dislocations and partials from GBs and explain the twinning behavior in NC metals. A simple, realistic model based on dislocations emission from GBs was constructed by Asaro et al. [35], in which the critical stresses needed to move a full dislocation and a partial are described respectively as follows:

$$\sigma_{\text{Full}} \propto \frac{\mu b}{d} \tag{1}$$

and

$$\sigma_{\text{Partial}} \propto \left(\frac{1}{3} - \frac{1}{12\pi}\right)\frac{\mu b}{d} + \frac{\gamma_{SF}}{b} \tag{2}$$

where μ is the shear modulus, b is the magnitude of Burgers vector of full dislocations, and γ_{SF} is the stacking fault energy (SFE).

The slip of partials in general triggers the formation of deformation twins and SFs that contribute to the plastic deformation of NC FCC metals. There is a double-inverse grain size effect on deformation twinning in NC metal with respect to the normal Hall-Petch (H-P) *d*-dependence, as uncovered in Ni [30] and Cu [31]. This nonmonotonic *d*-dependence of twinning is explained by Zhang et al. [31] via the stimulated slip model, involving the competing grain size effects on the emission of the first partial, and the plane-to-plane promotion of partial slip afterwards. Though this model was originally proposed to explain the H-P *d*-dependent twinning in CG metals (e.g., Ti), latter *in situ* TEM observations in stretched Au nanowires clearly demonstrated the stimulated slip of partials is operative at nanoregime [36]. Actually, just opposite to the trend of twinning, its reverse process, i.e., detwinning, also manifests the double-inverse *d*-dependence, as revealed in NT Ni [37].

It is conceivable that GB-mediated deformation become more important in NC metals due to a high density of GBs [38, 39]. Typically, this is expected to occur for grain sizes below 15 nm for most metals [38], because ordinary dislocation plasticity requires prohibitively high stresses to switch on, predicted from Eqs. (1) and (2). In this regime, GB-mediated deformation leads to material's softening or the so-called inverse H-P effect [40]. Given the pervasive dislocation nucleation and motion still prevails in such a small size-range, Carlton and Ferreira [41] established an elegant model based on the statistical absorption of dislocations by GBs to explain the inverse H-P effect, showing that the yield strength is dependent on strain rate and temperature and deviates from the H-P relationship below a critical grain size.

Building on these insights from NC metals, it is unexpected that Cu, even high SFE Ni, with submicron grains and a high density of nm-scale twin boundaries (TBs) exhibit the softening behavior deformed at RT. As a matter of fact, in NT FCC metals, the TBs not only serve as deformation barrier for dislocation transmission but also serve as dislocation sources as well as sinks [21, 42, 43]. Concomitantly, NT metals, e.g., Cu, also exhibit the size-dependent deformation mechanisms that transit from dislocation nucleation from steps on the TBs to TB/GB junctions at a critical twin thickness (λ_C), e.g., λ_C~18 nm for Cu [43], as shown in **Figure 2**. At this point, the classical H-P type of strengthening due to dislocation pile-up and cutting through twin planes transforms to a dislocation-nucleation controlled softening mechanism with TB migration resulting from nucleation and motion of partials parallel to the twin planes [44]. This mechanism transition size is quantitatively consistent well with the strongest size of ~15 nm determined by mechanical tests [21].

To summarize, NC metals exhibit size-dependent deformation mechanisms at different size regimes that involve GBs as the primary sources and sinks for dislocations as well as diffusive and sliding phenomena, that is to say, the size-dependence itself manifest strong size effects. This would inevitably affect the microstructural evolution and mechanical properties addressed below.

3.2. Microstructure evolution in nanostructured metals

Understanding the underlying physical mechanisms of grain growth/refinement in materials, in particular, for NT metals with simultaneous high strength and good ductility, to manipulate their microstructural stability for performance optimization is a grand challenge in the material community. It is well realized that the CG metals would shrink their grains, whereas

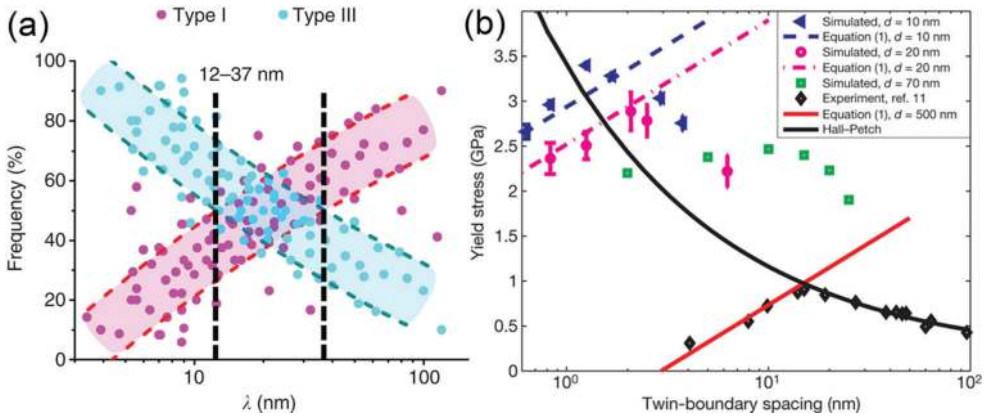

Figure 2. (a) Statistical distribution of two types of dislocations in NT Cu with different TB spacing λ during *in situ* deformations (left, figure is taken with permission from Ref. [43]). (b) Yield stress of NT Cu as a function of TB spacing λ at different grain sizes (right, figure is taken with permission from Ref. [44]).

the NC metals often coarsen their grains during plastic deformation even at low temperature. Similar phenomena were observed in NT metals and alloys, such as Cu. Therefore, it is naturally anticipated that for a metal it has a steady-state grain size (d_S) during plastic deformation, which was previously taken granted as a characteristic of each metal.

3.2.1. Steady-state grain size

So far, the steady-state grain sizes of metals have been thoroughly modeled in terms of various physical parameters by Mohamed [45] and further analyzed by Edalati and Horita [46] with respect to atomic bond energy and related parameters. The usage of applied stress (σ_a) in Mohamed's model [45] renders the roles of average internal stresses (σ_i) driving recovery or average effective stresses ($\sigma_e = \sigma_a - \sigma_i$) driving dislocation motion played in microstructural evolution during plastic deformation are indistinguishable. This treatment would miss some critical information about the physical mechanism(s) for microstructural evolution, which is unfavorable for us to design an engineering material with the steady-state grain size via tuning their initial microstructures and/or processing parameters. In the light of competition between average effective and internal stresses characterized by the stress ratio $\eta_{\text{Stress}} = \sigma_e/\sigma_i$, Li and coworkers [47] most recently constructed a new dislocation-based model to describe the steady-state grain size d_S for NS metals as

$$\frac{d_s}{b} = C\left[\frac{(2+\upsilon)M}{162\pi K b^2 \omega^2 \varphi}\right]\left(\frac{\mu b}{\gamma_{sf}}\right)\left(\frac{\mu}{\sigma_e}\right) \quad \text{for } (f = 0) \tag{3}$$

and

$$\frac{d_s}{b} = \frac{\sqrt{(1-f)^2 + C\frac{f}{\lambda}\frac{(4+2\upsilon)M}{81\pi K b\,\omega^2 \varphi}\left(\frac{\mu b}{\gamma_{sf}}\right)\left(\frac{\mu}{\sigma_e}\right)}}{2f}\frac{\lambda}{b} - \frac{1-f}{2f}\frac{\lambda}{b} \quad \text{for } (0 < f \le 1) \tag{4}$$

http://dx.doi.org/10.5772/66598

where C is a stress-dependent coefficient in-between the growth rate C_1 and the refinement rate C_2, and a useful representation of the coefficient C as a function of σ_e, consisting of C_1 and C_2 below and above the internal stress σ_i, respectively, is $C = ((C_1 + C_2)/2) - ((C_1 - C_2)/2)\,\mathrm{erf}((\sigma_e - \sigma_i)/\Delta)$, Δ is a measure of the extent of the transition region, M is the Taylor factor, μ is the shear modulus, υ is Poisson's ratio, φ *is* the misorientation angle between neighboring grains, ω represents the linear atomic density of the dislocation line, f is the number fraction of nanotwins, and K is a constant ($K = 1$ for screw dislocations and $K = (1 - \upsilon)$ for edge dislocations). This model captures well with the steady-state grain size d_S obtained from free-standing NS Ni foils with λ = 38 nm at the steady-state creep stage tested at RT, as shown in **Figure 3**. Interestingly, by postmortem transmission electron microscopy (TEM) observations, Li et al. [47] uncovered that the ED NT Ni foils (with a strong (111) peak and followed by (200) and (311) peaks) prefer to display grain coalescence at low stress ratios $\eta_{\mathrm{Stress}} < 1$, while they prefer to display grain refinement at stress ratios $\eta_{\mathrm{Stress}} > 1$ during the creep test. When the effective stress balances the internal stress, i.e., $\eta_{\mathrm{Stress}} = 1$, these NT Ni foils sustain the stable microstructures. Note that the stress ratio itself is strongly temperature- and strain rate-dependent, in that the internal stress σ_i has contained the contribution of the thermal component. In their work, the grain refinement/growth in the NT Ni is achieved by twinning- or detwinning-mediated mechanism via dislocation-boundary interactions. Similar phenomena in cyclically compressed bulk NC Cu with an initial d of ~25 nm and in fatigued ultrathin Au thin films with an initial d of ~19 nm were observed by Hu et al. [34] and Luo et al. [48], respectively, at RT. The underlying reasons for grain growth are the excessive energy of GBs/TBs and randomly orientated grains [49] in these Ni and Cu nanostructures synthesized by the nonequilibrium deposition.

3.2.2. Mechanisms of grain growth and grain refinement

Traditionally, mechanistic descriptions that have been developed to describe NC metals have generally considered the GBs to be stable and immortal obstacles to dislocation motion, whereas there are numerous evidences that suggest that this is not always the case [4–7]. Such materials are often unstable: The NC grains tend to merge and grow larger as subjected to heat or stress. Indeed, *in situ* nanoindentation of ultrafine-grained (UFG)/NC Al films deposited on specially designed Si wedges demonstrated rapid GB migration and coalescence during deformation [4]. Another representative study has reported the grain growth of UFG/NC Cu near the indented region during microhardness testing at both cryogenic temperature and RT by Zhang et al. [5]. They surprisingly uncovered that the grain growth was found to be faster at cryogenic temperature than at RT, implying that the grain coarsening process is driven primarily by stresses rather than diffusion. Gianola et al. [6, 7] concluded that stress-driven grain growth appears to have preceded dislocation activity and involved GB migration and grain coalescence and becomes an active RT deformation mode in abnormally ductile NC Al thin films, based on coupled microtensile thin-film testing, *in situ* synchrotron diffraction experiments, and postmortem TEM observations. However, the twinning-mediated grain grow mechanism unveiled in stretched NT Ni [37, 47] and compressed NT Cu [34] is radically different from these grain growth mechanisms aforementioned above.

Figure 4 shows the atomic evidence of twinning-mediated grain growth in NT Ni, essentially being the consequence of nanotwin-assisted GB dissociation and local grain coarsening. Because the localized misorientation between two adjacent grains G1 and G2 can be reduced

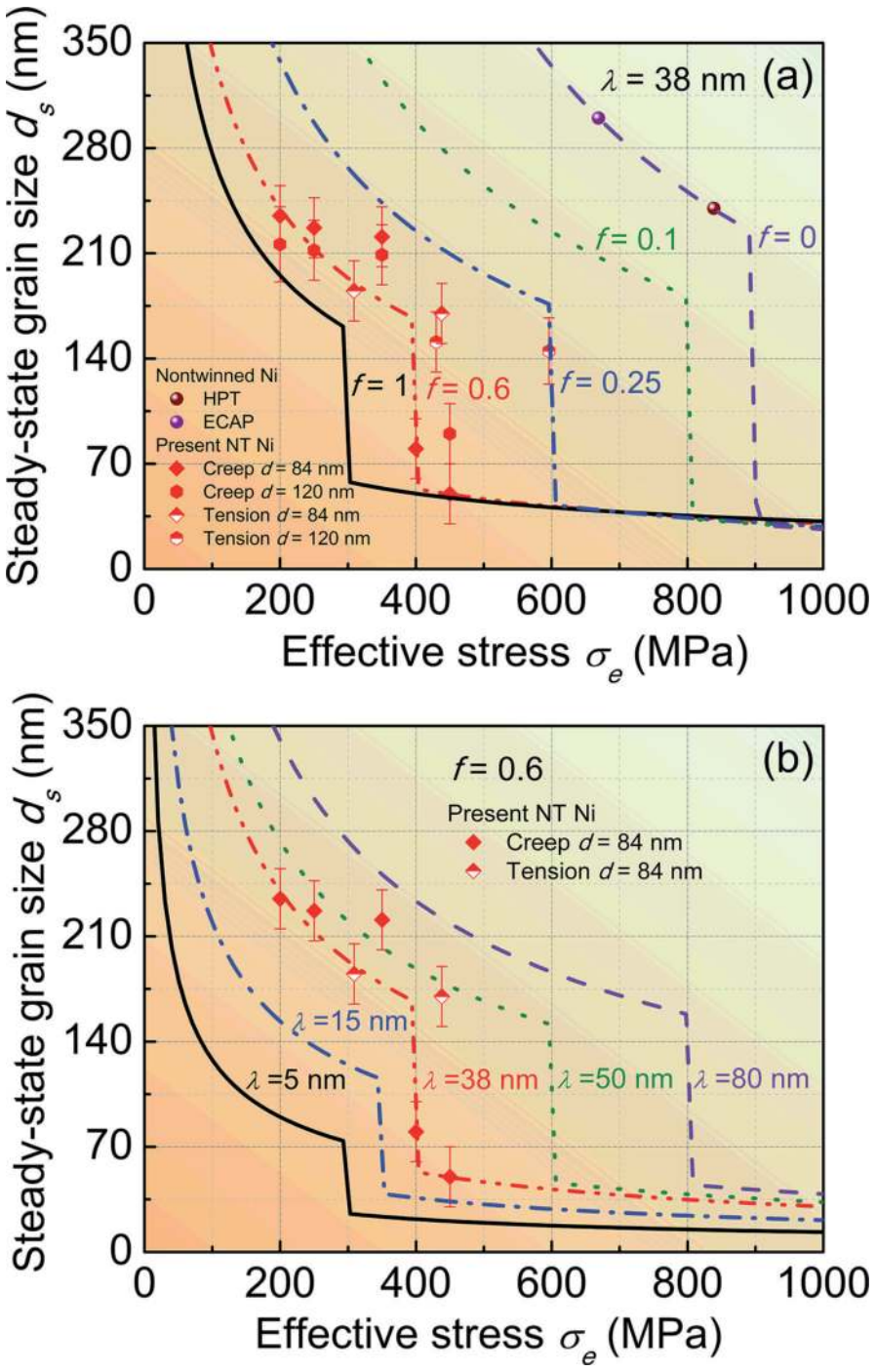

Figure 3. (a) Calculated steady-state grain size ds as a function of average effective stress σ_e in nanograined Ni with different twins' fraction f (a) and twin thickness λ (b). Figure is taken with permission from Ref. [47].

http://dx.doi.org/10.5772/66598

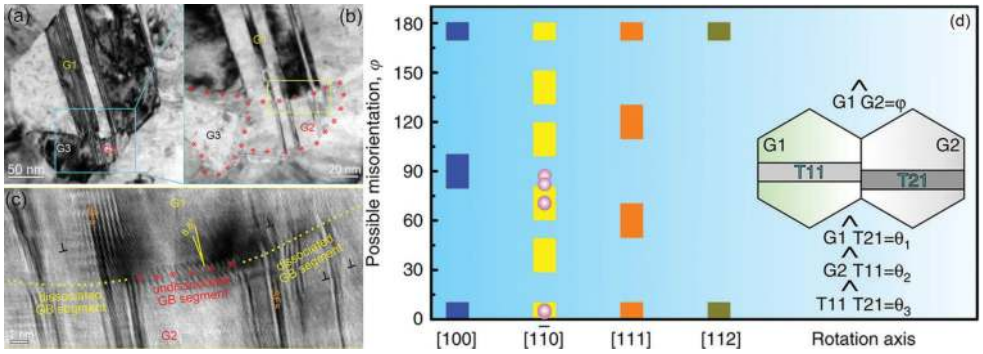

Figure 4. The TEM images showing nanotwin-assisted grain growth occurred among three grains (labeled as G1, G2 and G3, respectively) in NT Ni after creep. (b) is the magnified view of blue rectangular region in (a) and (c) is the magnified view of yellow rectangular region in (b) showing grain coalescence between G1 and G2 (left, figure is taken with permission from Ref. [47]). (d) Possibility for nanotwin-assisted grain coalescence. Possible misorientation angle (ϕ) suitable for nanograins G1 and G2 coalescence induced by the present nanotwin-assisted mechanism under different rotation axes <*hkl*> (right, figure is taken with permission from Ref. [48]). The inset shows all the misorientation angles among grains and twins.

by twinning, leading to some parts of G1 being transformed into G2, thus some localized segments of GB coalesce and disappear, see **Figure 4(b)** and **(c)**. Consequently, the repetitive formation of nanotwins induces some local segments of a high-angle GB are transformed into low-angle GB segments by storage of residual dislocations generated from dislocation reactions [37]. These recurrent interactions between partials/twins and GBs would facilitate the two adjacent nanograins to gradually coalesce into one larger grain with nanotwins. Moreover, there is a great possibility for the present mechanism to occur in G1/G2 with different mutual misorientation (φ) through the rotation around four typical low-index symmetric axes <*hkl*>, in particular, for φ<*111*> (φ = 0–10°, 50–70°, 110–130°, and 170–180°) and φ<*110*> (φ = 0–10°, 29–48.9°, 60.6–80.5°, 99.5–119.4°, 131.1–151°, and 170–180°) [48], as shown in **Figure 4(d)**.

Figure 5 displays the TEM observation of detwinning-induced refinement of grains in NT Ni, achieved by interplay between partials and primary TBs. Two typical examples of the interactions are presented in **Figure 5(b)** and **(c)**. It appears that the atomic arrangement is distorted at the intersection region of twins, see **Figure 5(b)**. The presence of SFs in the primary twin implies the gliding of partials created by dislocation-TB reactions [50]. In **Figure 5(c)**, these Shockley partials glide parallel to the CTB, rendering detwinning of the primary twin, as observed in the twins crossed region of R4. As deformation proceeds, these partials stimulate twinning process, resulting in twin interactions to produce abundance of sessile dislocations. As a consequence, CTBs lose their coherency and transform into conventional GBs [51]. Obviously, this mechanism is parallel with other mechanisms for nanoscale structural refinement via twin/matrix lamellae in various FCC metals are identified, such as fragmentation of T/M lamellae, twins intersection, and shear banding [52].

3.3. Size effects on the mechanical properties

Mechanical properties of nanoscale structures are well known for deviating from their CG counterparts, exhibiting size effects across a wide range of properties. These NS metallic

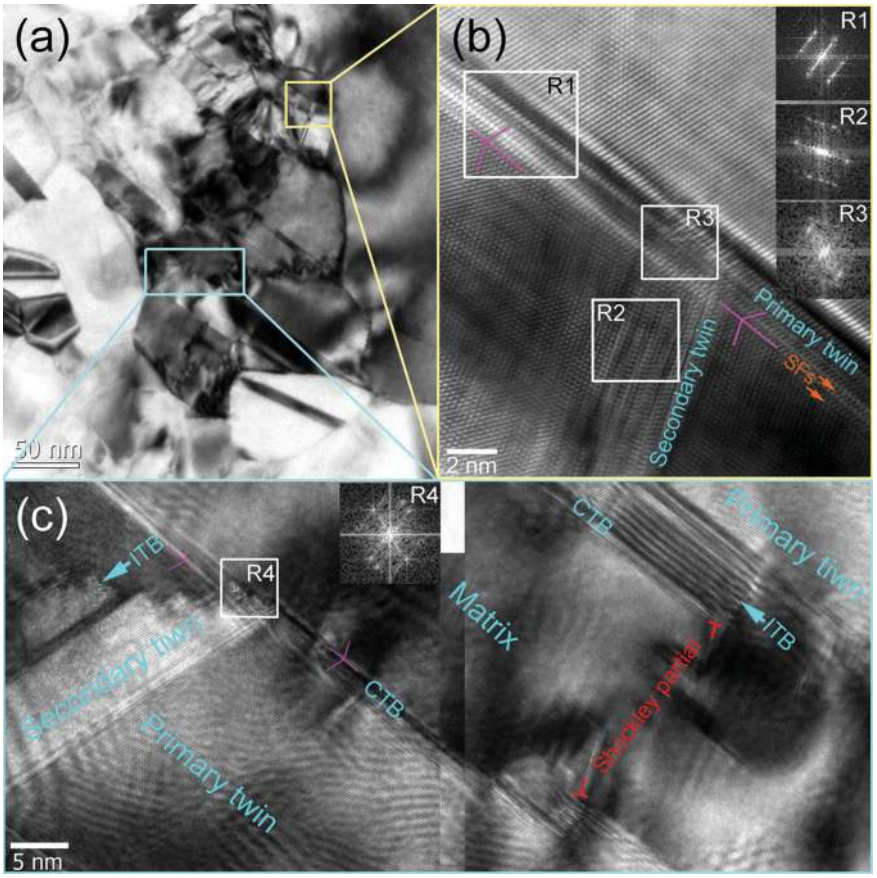

Figure 5. The TEM images showing the GB formation for grain refinement via detwinning-induced twin interactions in NT Ni after creep. Figure is taken with permission from Ref. [47].

materials generally fall under the banner of "smaller is stronger." The result of this size effect is that NS thin films often exhibit mechanical properties of an increased magnitude: typically the yield strength, strain rate sensitivity (SRS), and fatigue lifetime all increase with respect to the accepted bulk values.

3.3.1. Strength and ductility

A striking feature of NS metals is their extraordinary strength compared to corresponding bulk materials. The dependence of measured yield strength σ_y of either substrate supported [23, 53–57] or freestanding [56] Cu on film thickness h and on grain size d are summarized and shown in **Figure 6(a)** and **(b)**, respectively. It seems that, similar to their bulk NS counterparts, σ_y of Cu thin films also monotonically increases with reducing d and shows some-

http://dx.doi.org/10.5772/66598

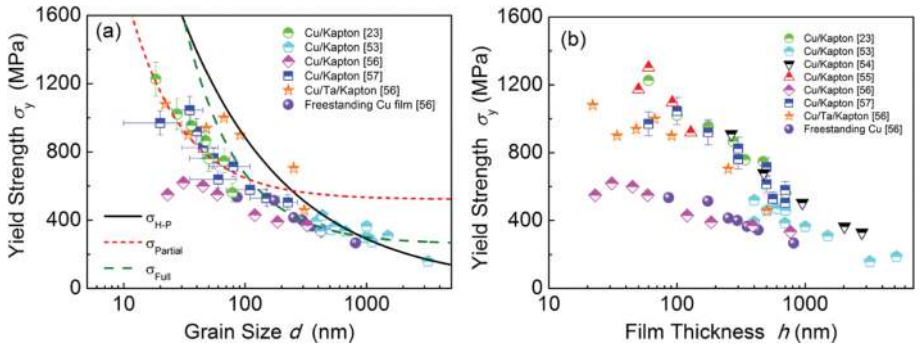

Figure 6. The dependence of yield strength of Cu thin films as a function of (a) grain size *d* and (b) film thickness *h*. The lines in (a) are predictions of yield strength from the H-P relationship, partial dislocation model (Eq. (1)) and full/perfect dislocation model (Eq. (2)), respectively.

what drop until *d* reduces down to ~20 nm, as shown in **Figure 6(a)**. In this strengthening regime, σ_y obeys the empirical H-P relationship, i.e., $\sigma_y \propto d^{-0.5}$, at $d \geq$ ~800 nm. Below this grain size, the strength of UFG/NC Cu thin films can be well captured by Eqs. (1) and (2). Also, **Figure 6(b)** clearly shows σ_y increases with decreasing *h* down to nanoregime and appears to drop slightly between 20 and 50 nm thickness. In general, *d* trends to scale with *h*. Thus, the strengthening of Cu thin films results from the constraints of both *d* and *h* on dislocation nucleation and motion.

The attainment of both strength and ductility is a vital requirement for most structural materials; unfortunately these properties are generally mutually exclusive. This general belief holds true for these NS metallic thin films/foils, such as Cu and Ni. For example, Niu et al. [23] studied the tensile ductility of NC Cu thin films with thickness spanning from 60 to 700 nm by characterizing the critical strain to nucleate microcracks, and revealed the fashion of "smaller is stronger and smaller is less ductile." The limited tensile ductility in NS thin films can be ascribed to the lack of strain hardening and grain geometry. In particular, the NC thin films with columnar grains are more favorable to exhibit quite limit uniform tensile elongation, because the insufficient room in NC grains does not permit involving intragranular dislocation interaction and entanglement and cracks are easier to propagate along columnar GBs [58]. This intrinsic limitation promotes plastic instabilities such as necking or cracking.

By far, three available strategies are presented that demonstrate enhancement of ductility in NC metals, including engineering grain-size distributions [59], embedding growth nanotwins [21], and designing high twinnability NC metals [60]. Gianola et al. [6] has uncovered that the stress-assisted grain growth has a dynamic effect on the macroscopic mechanical properties of free-standing NC Al thin films; extended ductility can be realized along with a concurrent loss in strength in comparison to tests in which no grain growth was observed. Therefore, this twinning-mediated grain growth mechanism unveiled in NT Ni [37, 47] seems to synergically combine the merits of (deformation/growth) nanotwins and grain growth mentioned above, being a novel and promising method to enhance the tensile ductility of NS metals for their performance optimization.

3.3.2. Strain-rate sensitivity

The plastic deformation kinetics in NS metals could be investigated to shed light on the strength-ductility tradeoff. It is well known that a material's strain rate dependence is usually quantified through the power law relationship: $\sigma = \sigma_0 \dot{\varepsilon}^m$ [61]. The strain-rate sensitivity (SRS) of a material can be characterized by two key kinetic signatures of deformation mechanisms, i.e., SRS index (m) and activation volume (V^*), both of which correlated via the expression $m = \frac{\partial \ln(\sigma)}{\partial \ln(\dot{\varepsilon})} = \frac{\sqrt{3}\, k_B T}{\sigma V^*}$. The former characterizes the rate-controlling process, while the latter characterizes deformation kinetics in a metal. From a series of experiments, the SRS m is summarized **Figure 7(a)** and **(b)** for UFG/NC nontwinned [62–69] and NT [37, 70, 71] FCC metals (i.e., Cu and Ni). **Figure 7(a)** shows that m for several typical small-scaled Cu materials (e.g., NC Cu, single and multicrystalline Cu micropillars) increases monotonically with decreasing their *size parameters*, with $m > 0.01$ for small-scaled NS Cu. This trend is similar to the d-effect in other nontwinned FCC metals, such as Ni [64–67], and to the λ-effect in NT Ni foils [37, 71] and bulk NT Cu [70] that are presented in **Figure 7(b)**. The large m achieved in both cases can facilitate suppressing localization at high deformation rates. In contrast, the BCC metals in general exhibit the reduced m with decreasing d [62, 72]. The fundamental difference between FCC and BCC metals can be attributed to their different dislocation core structures.

Insight into the dominant deformation mechanism is often interpreted in terms of the values of activation volume V^* for plastic deformation. In CG FCC metals, a typical rate-determining process, such as the intersection of forest dislocations, gives a large V^* of the order of several hundred to a few thousand b^3 [61, 70]. At another extreme, GB sliding or GB diffusion mediated creep (Coble creep) gives a small V^* of less than $1b^3$. When the V^* is between $1b^3$ and $100b^3$, the rate process typically involves cross-slip or dislocation nucleation from boundaries [70]. Recent findings have shown that there is linear relationship between the activation volume V^* and *size parameters*, such as grain size d, twin thickness λ and pillar diameter φ in the log-log plots [68, 69].

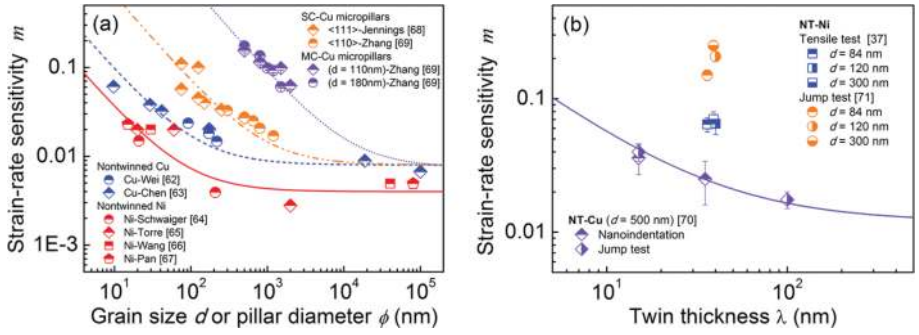

Figure 7. Strain-rate sensitivity of FCC Ni and Cu metals as a function of (a) grain size (d) or pillar diameter (ϕ) and (b) twin thickness (λ), summarized from available literatures [37, 62–71]. All the curves are visual guides.

http://dx.doi.org/10.5772/66598

3.3.3. Mechanical fatigue lifetime

The continuing trend of miniaturizing materials in micro- and nanodevices has led to a strong demand for understanding the complex fatigue properties of NS thin films to tailor their internal features to guarantee their reliability. Zhang and coworkers [57] investigated the fatigue behavior of NC Cu thin films with thickness spanning from 60 to 700 nm on compliant substrates by *in situ* measure the change of electrical resistance with the number of cyclic loading, by adopting the method proposed by Sun et al. [24]. **Figure 8(a)** clearly shows the dependence of fatigue lifetime (N_f) of NC Cu films on h at different strain ranges ($\Delta\varepsilon$). It is found that there is a maximum N_f at the critical thickness of h = 100 nm, above which N_f monotonically increases with reducing h at a constant $\Delta\varepsilon$. While below this critical thickness,

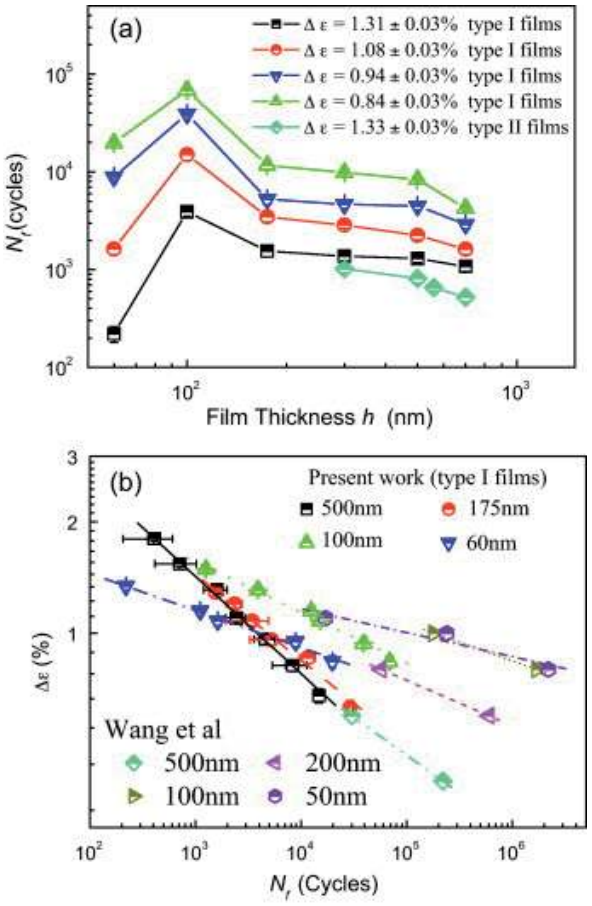

Figure 8. (a) Dependence of fatigue lifetime N_f on strain range $\Delta\varepsilon$ as a function of film thickness h for Cu thin films, respectively. (b) A comparison of the relationship of $\Delta\varepsilon - N_f$ in Cu thin films with different thickness h. Figure is taken with permission from Ref. [57].

N_f decreases with further reducing h. This is caused by the good combination of high strength (~1050 MPa) and suitable ductility (~5.5%). Luo et al. [48] recently also pointed out that in addition to the potential contribution from the high strength of nanograins (of Au), notable improvement in fatigue properties may be closely associated with twinning-mediated grain growth. For a given h, a higher $\Delta\varepsilon$ leads to a smaller N_f of the Cu thin film. Moreover, all Cu thin films exhibit the dependence of N_f on $\Delta\varepsilon$ that could be well described by the well-known Coffin–Manson relationship: $(\Delta\varepsilon/2) = \varepsilon_f(2N_f)^c$, where ε_f and C are the fatigue ductility coefficient and exponent, respectively, as shown in **Figure 8(b)**. Accordingly, with reduction in h from 700 nm with d = 220 nm to h = 60 nm with d = 20 nm, the surface damage morphologies change from extrusion/intrusion to intergranular cracks, due to the transition of deformation mechanism from dislocation-based to GB-mediated. In other words, with decreasing *size parameters* the localized accumulation of plastic strains within grains is hindered and the GBs take over as the preferred site for damage formation, implying the availability and activation of bulk dislocation sources become more limited in NC metals. This is consistent with the postmortem TEM observations by Zhang et al. [73].

4. Grain boundary segregation in nanocrystructured metallic materials

During the past two decades, NS metallic materials have received considerable attention owing to their unique, often desirable properties for engineering applications, whereas they manifest two adverse properties: low ductility and microstructural instability as mentioned earlier. This is because the high energy GBs associated with high mobility can absorb abundant dislocations, resulting in low dislocation storage inside grains [2, 3]. Therefore, a universal strategy to remarkably enhance/improve the mechanical properties and thermal stability of these NS materials is to manipulate their multihierarchical microstructures by embedding atoms/clusters or nanoparticles in grain interiors to increase dislocations storage and at GBs to prevent grain growth by reducing GB mobility [74]. Fortunately, alloying opens an available avenue to achieve such an idea about microstructure-sensitive design to improve materials' properties by tuning solute distributions, in particular, GB segregation, in NS thin films to achieve thermodynamically stable or metastable states [75–81]. The addition of an alloying element has fundamental thermodynamic implications for NC metals, which can explain the unique ability of alloyed systems to exhibit fine-grained structures [8–13, 75–81]. Specifically, Schuh's group [11–13] recently developed a theoretical framework for a regular NC solution (RNS) that incorporates GB segregation and further built an insightful nanostructure stability map for design alloys with positive enthalpy.

In what follows, we mainly address alloying effects on microstructural evolution on the one hand, and on the mechanical properties on the other in three categories of typical binary Cu-based film systems, i.e., Cu-Zr, Cu-Al, and Cu-W. This division of three typical binary systems is based on the consideration of mixing enthalpy (H_{mix}) and the conventional bulk binary diagram under equilibrium states (at RT), and can be extended to other systems like Ni-based binary alloy.

http://dx.doi.org/10.5772/66598

4.1. Alloying effects on microstructure and mechanical properties in the Cu-Zr model system

In such system that has a very negative enthalpy of mixing, only elemental Cu and intermetallic Cu-Zr phases coexist at room temperature under equilibrium state. However, nonequilibrium MS can result in the coexistence of solute (Zr) atoms/clusters, Cu-Zr intermetallic particles, and Cu-Zr amorphous phase in the as-deposited alloyed thin films to achieve multihierarchical microstructures, thereby facilitating the combination of high strength and ductility.

Zhang et al. [82] systematically investigated the microstructural evolution, mechanical properties, and deformation mechanisms of NS Cu thin films alloyed with Zr. It is found that Zr addition significantly changes the microstructures of NS Cu thin films. A strong (100) texture observed in the pure Cu film is strongly suppressed while the (110) texture is favorably promoted in the Cu-0.5 at.% Zr and Cu-2.0 at.% Zr films. When the Zr content is up to 8.0 at.%, the (100) and (110) peaks disappear and the (111) peak is also highly weakened, associated with an obvious amorphization tendency. The underlying reason for the change of crystallographic orientations of Cu-Zr alloyed thin films can be attributed to the effect of reduced GB energy caused by GB segregation on the competition between surface energy and strain energy [82].

Along with the crystallographic orientations change, the GB microstructures of Cu-Zr alloyed thin films also change with Zr doping, as displayed in **Figure 9**. Zhang et al. [82] uncovered that in the Cu-0.5 at.% Zr film, some nanosized $Cu_{10}Zr_7$ precipitates occasionally observed at the GBs, as indicated in **Figure 9(a)** and **(b)**, associated with notable GBs segregation of Zr,

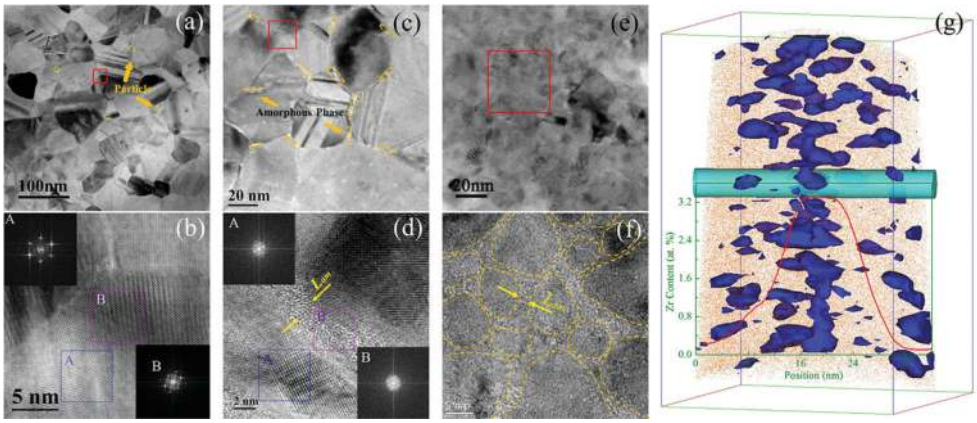

Figure 9. Representative TEM and HRTEM images demonstrating the architectured microstructures in the Cu-0.5 at.% Zr (a, b), Cu-2.0 at.% Zr (c, d), and Cu-4.0 at.% Zr (e, f) films. (g) The 3DAP image of the Zr segregation at the GB and the variation of concentration of Zr at different position along the line. Figure subparts (a–f) are taken with permission from Ref. [82].

see **Figure 9(g)**. Actually, besides having an important role in reducing GB energy, GB segregation can drive the formation of new interfacial structures at the GBs. In the Cu-2.0 at.% Zr film, discontinuous amorphous phases are frequently observed at the GBs, as indicated in **Figure 9(c)** and **(d)**. When the Zr addition is up to 4.0 at.%, GBs are unclear and continuous amorphous phase is distributed along the GBs, as shown in **Figure 9(e)** and **(f)**. Their TEM findings are consistent well with the XRD results mentioned above that Zr addition in host metal of Cu tends to induce amorphization.

Apart from the amorphization tendency and grain refinement, another significant change in microstructure caused by the Zr addition is the twinnability in the Cu films. Somewhat soluble Zr atoms reduce the SFE and thus increase twinning propensity, while excessive Zr addition induces sharply reduced twinning propensity. The dependence of twinnability on Zr addition was rationalized from the mechanisms of annealing twins by these authors [82], including (i) the successive and random emission of Shockley partials from GBs, and (ii) the GB migration mechanism accompanied with twins formation. However, the twin thickness monotonically decreases with increasing Zr contents in a fashion as same as the grain size. Furthermore, Zhang et al. [82] unambiguously demonstrated that the architectured microstructures, in particular, the GB complexions, significantly influence the mechanical properties, such as strength/hardness, ductility, and fatigue lifetime of NS materials, addressed below.

The most striking finding in their experiments [82] is that Zr addition offers exceptionally high values of both strength and ductility for the NS Cu thin films and both the strength/hardness and tensile ductility reach peak values at 0.5 at.% Zr addition, as shown in **Figure 10**. With further increasing Zr contents, the hardness shows slow reduction whereas the ductility exhibits sharp reduction. The high strength stems from various contributors, including solid solution (clusters) strengthening [83], GB solute segregation [84], Zener drag effect [85, 86], and GB/TB strengthening [3], in addition to the contribution from amorphous phase in high Zr contents samples [87–90]. The remarkable enhancement in ductility of the Cu-0.5 at.% Zr film stems from the stress-driven grain growth via twinning mechanism, displayed in **Figure 11**, like that in the pure ED Ni foils [37, 71] mentioned in Section 3. This is an indirect effect of Zr doping that benefits the emergence of (110)-oriented grains, leading to random crystallographic orientations, i.e., coexistence of (111), (100), and (110) grains, whose cooperative interaction is known to facilitate grain coarsening. This new finding in Cu-0.5 at.% Zr thin film challenges the conventional wisdom that improving the strength of a metal alloy is always a tradeoff that results in a loss of ductility—the property that allows a metal to deform without fracture.

Also, Zhang and his colleagues [82] explored the mechanical fatigue properties of these deposited Cu-Zr alloyed thin films. The NS Cu-Zr thin films were cyclically strained under different total strain ranges and the strain range $\Delta\varepsilon$ versus lifetime N_f curves were experimentally determined for the Cu films with different Zr addition, as shown in **Figure 12**. All these films exhibit the dependence of N_f on $\Delta\varepsilon$ that could be well described by the Coffin-Manson relationship: $(\Delta\varepsilon/2) = \varepsilon_f(2N_f)^C$, where ε_f and C are the fatigue ductility coefficient and exponent, respectively. At the strain range of 0.5–3.0, the Cu-0.5 at.% Zr film always displays

http://dx.doi.org/10.5772/66598

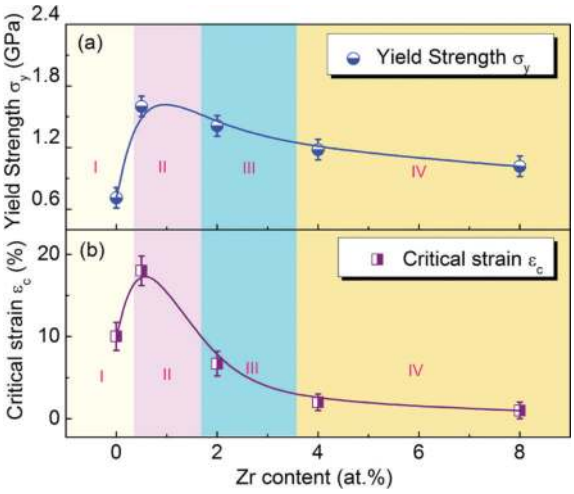

Figure 10. Dependence of yield strength ($3\sigma_y$ = Hardness) (a) and ductility characterized by the critical strain to nucleate microcracks (ε_C) (b) on Zr content. Four regimes (I, II, III, and IV) are divided which correspond to four different microstructures in the Cu, Cu-0.5 at.% Zr, Cu-2.0 at.% Zr, and Cu-Zr (Zr > 4.0 at.%) films, respectively. Figure is taken with permission from Ref. [82].

the greatest fatigue lifetime among all the films while the pure Cu film manifest the shortest one. The fatigue resistance of NS Cu films is notably enhanced via either GB segregation of Zr atoms/precipitates or amorphous phase formation of Cu-Zr, resulting in retardation of fatigue damages. Different from the uniaxial tension test, the amorphous phase plays a crucial role in the prolonged fatigue lifetime through depressing microcrack nucleation and through the arrest of intergranular cracks. Although previously atomistic simulations [87] showed that the nanoscale amorphous intergranular phase as a structure feature plays a critical role in toughening NS materials, as verified in crystalline/amorphous Cu/Cu-Zr nanolaminates [88–90], the presence of amorphous phase in Cu-Zr alloyed thin films apparently deteriorate their tensile ductility, as least at high Zr additions. This GB complexion effect on the mechanical properties is quite interesting and requires further work to reconcile the current discrepancy. Still, postmortem TEM observations in the fatigued Cu-Zr thin films verified that the occurrence of stress-driven grain growth under fatigue conditions, as same as that in tensile deformation. These findings show that the fatigue of thin metallic films remains a very attractive field of research due to the possible complex interplay of the possible deformation and fracture mechanisms.

4.2. Alloying effects on microstructure and mechanical properties in the Cu-Al model system

In this miscible system with H_{mix} close to zero, solute (Al) has a significant solid solubility in the host metal (Cu), and consequently, only a weak segregation tendency. The miscible solutes inside grains, in principle, allowing certain material properties to be finely

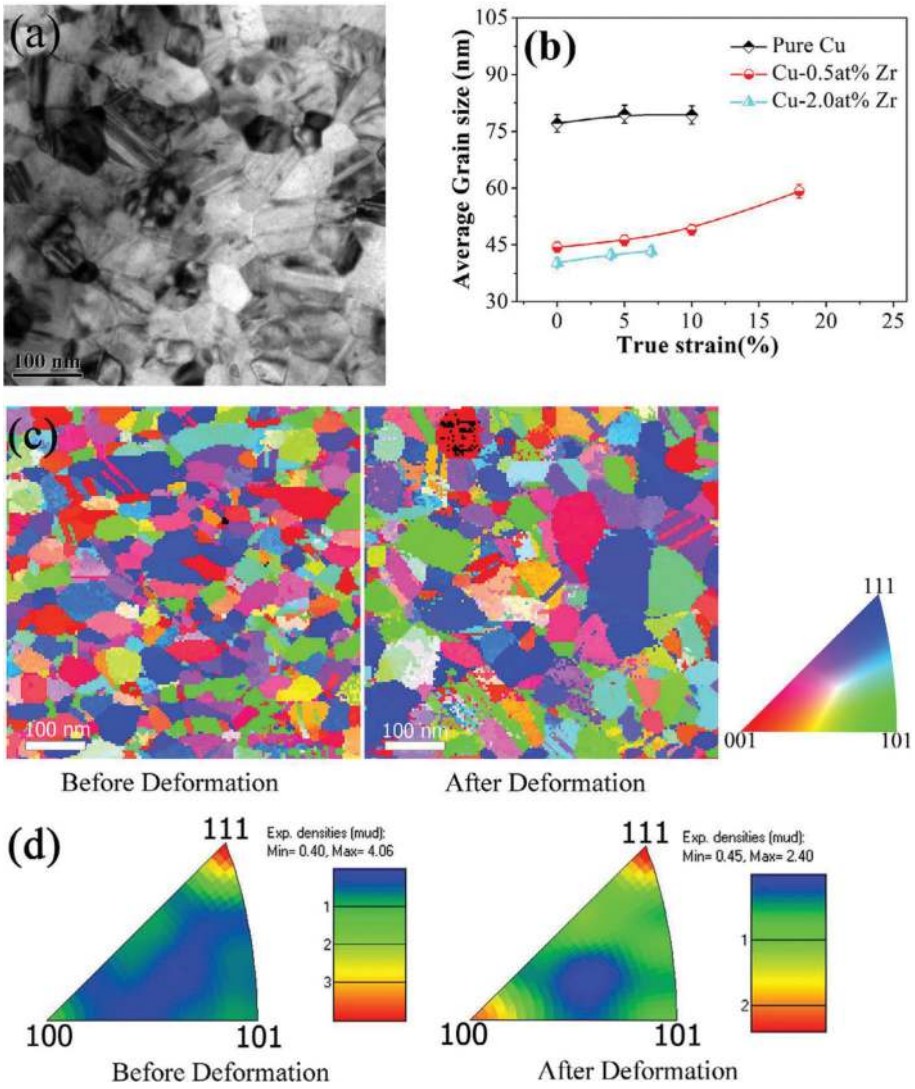

Figure 11. (a) A representative planar TEM image showing the grains in Cu–0.5 at.% Zr film stretched to 18% to demonstrate the increase in grain size. (b) Statistical results on the grain size evolution with applied strain in the pure Cu, Cu-0.5 at.% Zr and Cu-2.0 at.% Zr films. (c) Representative color-coded inverse pole figure maps from the Cu-0.5 at.% Zr film before deformation (left) and after stretching to ε_C (right), respectively, with color coding at the lower right corner. Grain growth can also be observed by comparing the images before and after deformation. (d) Corresponding orientation distributions presented as an inverse pole plot, which can be used to show the variation in orientation. Figure is taken with permission from Ref. [82].

tuned: The nucleation of partial dislocations, for instance, is stimulated by miscible solutes through markedly decreasing the SFE of the host metal [91]. For example, as NS Cu films is alloyed with Al, more nanotwins with thinner thickness are observed in the as-deposited Cu-Al thin films with lower SFE or higher fraction of Al [92, 93].

http://dx.doi.org/10.5772/66598

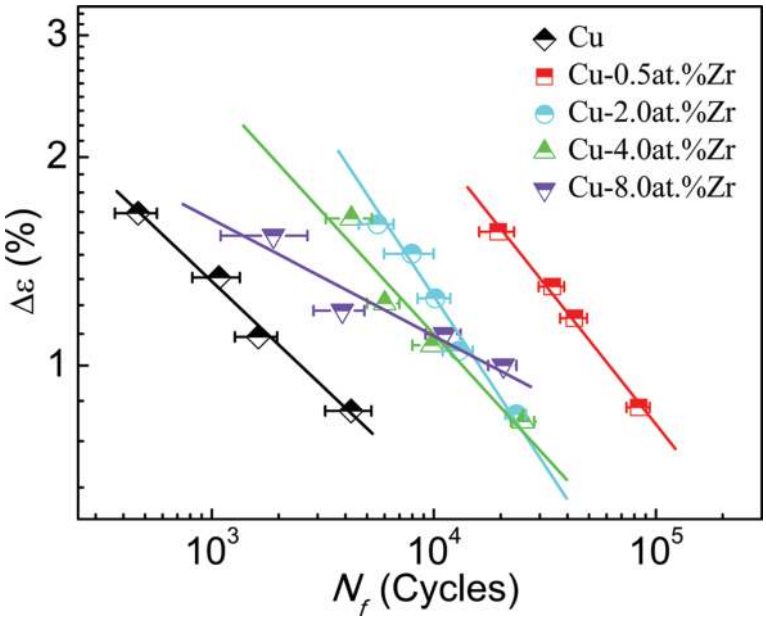

Figure 12. Dependence of the fatigue lifetime (N_f) on the strain range ($\Delta\varepsilon$) for pure Cu and Cu-Zr alloyed thin films. Figure is taken with permission from Ref. [82].

Recently, NS Cu films with different Al additions (0, 1, 5, and 10 at.%) were prepared by MS to investigate the effect of lowering SFE on microstructures and mechanical properties by Zhang et al. [92]. It is found that the Al addition motivates nanotwin formation, and promotes (111) but depresses (100) texture. With increasing Al contents, along with the refinement of grains, the morphologies of nanotwins transformed from parallel nanotwins in pure Cu to multiple nanotwins in Cu-5 at.% Al and to intersected nanotwins network in Cu-10 at.% Al, as shown in **Figure 13** as insets. Concomitantly, these Cu-Al alloyed thin films exhibit increased strength/hardness and reduced ductility with Al contents, namely, the Cu-Al films suffer from the strength-ductility tradeoff. Nevertheless, a good combination of hardness/ductility (6.2 GPa/6.3%) is achieved in the Cu-5 at.% Al film, which can be ascribed to the combined effect of texture and nanotwins [92]. At the same time, Heckman and coworkers [93] synthesized fully NT Cu-Al alloyed thin films with columnar grains and showed an increased strength of up to ~1.5 GPa that was closely related to the decrease in grain size or increase in Al content. Moreover, the ductility could be improved with decreasing the nanotwin thickness [93]. Except for the amorphous phase reinforced effect, all the strengthening mechanisms mentioned in the Cu-Zr model system play important roles in the strength of Cu-Al system. Also, Schäfer et al. [91] suggested that the details of the element distribution in the GBs are of great importance for the yield strength of the miscible alloy. The initial energetic state of the GB controls the barrier for the onset of deformation mechanisms, which is correlated to the maximum strength. Specifically, the formation of stacking faults and coherent TBs leads to material softening at high strains, because they provide additional dislocation sources. This is similar to that in pure Cu [21] and Ni [37] with very thin twins.

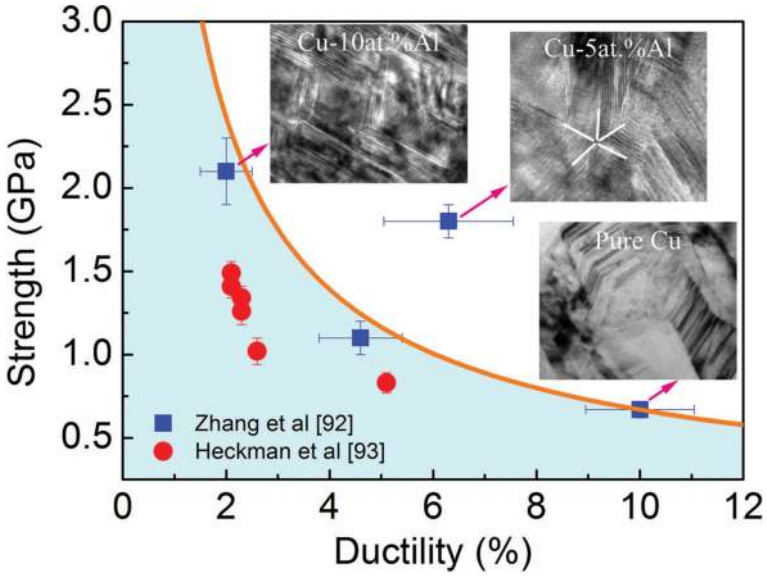

Figure 13. The strength-ductility tradeoff in Cu-Al alloyed thin films from literatures [92, 93]. Insets are the corresponding internal feature of Cu-Al films prepared by Zhang et al. [92].

In order to investigate the GB character evolution associated with the observed grain growth in this binary system, Brons and Thompson [94] carried out the *in situ* TEM observations on a sputter-deposited Cu-20 at.% Ni alloyed film that was annealed within a TEM equipped with the PED. It is found that alloying leads to a preferential evolution of particular grains. The onset of annealing resulted in multiple textures and grain growth evolution. It is clear from these results that significant differences in coincidence site lattice (CSL) boundary evolution occurred with the addition of Ni to the Cu thin film. The boundary fraction of Σ9, for the alloy film, was a factor of five larger than the pure Cu film and these boundaries were notably bounding several (but not all) of these larger grains. Additionally, Σ11 boundaries showed an increase in their fraction as compared with the elemental Cu grain growth evolution. They proposed that the Ni additions occupied subinterface sites as a result of higher surface tension of Ni which impedes other CSL boundaries motion [94]. Though solute segregation has been proposed as an efficient and effective way to stabilize NC grain structures (e.g., in Ni-W films [83]), solute preference to specific CSL boundaries can result in abnormalities in grain growth and lead to destabilization of the grain structure (e.g., in Cu-Ni films [94]). These results suggest that the GB segregation is much more complex. However, most previous numerical studies arbitrarily place solute atoms at GBs to determine their effect on GB energy [95–98], only some limited studies have been conducted to study the correlation between the CSL boundaries and solute segregation [94, 99, 100]. Therefore, further works are urgently needed to focus on how GB character is influenced with solute alloying.

http://dx.doi.org/10.5772/66598

4.3. Alloying effects on microstructure and mechanical properties in the Cu-W model system

It is well recognized that the Cu-W system is an essentially immiscible one characterized with a quite positive H_{mix} of about +22 kJ/mol. There does not exist any Cu-W compound in its equilibrium phase diagram. Actually, for the most studied immiscible binary alloyed films (such as Cu-W [101], Cu-Cr [102], and Cu-Ta [103]), nonequilibrium NS alloys, i.e., supersaturated solid solutions (SSSs), can be obtained by MS. Compared with the elemental (Cu) thin films, it is normally expected that the marked solute segregation that alters GB characters could occur and the solute drag effect could yield smaller grains [8, 12], both of which affect the propensity of nanotwin formation in binary Cu-based thin films.

Vüllers and Spolenak [101] recently prepared the "immiscible" Cu-W thin films with different W contents on silicon substrates using MS, and clearly demonstrated that these NC Cu-W thin films transit from the SSSs in a metastable as-deposited state to fully phase separated interpenetrating networks after annealing at 750°C, as shown in **Figure 14**. The W additions notably change the microstructural configurations of crystalline Cu thin film that has a distinctive columnar superstructure consisting of large numbers of partially even equiaxed grains and occasionally occurring twins, in the as-deposited state. While the columnarity dominant for pure Cu is still present in a 5 at.% W film, the subordinate structure making up the single columns in the pure Cu cross-section cannot be observed any longer. Films of higher W contents up to and around 30 at.% W do not exhibit a distinct crystalline structure in the as-deposited state. Subsequently, they measured the hardness and modulus of these Cu-W thin films as function of the W content at different states. It can be deduced that W content strongly influences the film's mechanical performance. As a whole, both hardness and modulus increase with increasing W contents, as shown in **Figure 14**. However, they did not perform quantitatively calculation of the strength of Cu-W thin films. Harzer et al. [102] quantitatively evaluated the hardness of metastable Cu-Cr alloyed thin films which are stable below ~170°C, and further correlated it with respect to film compositions and grain sizes in

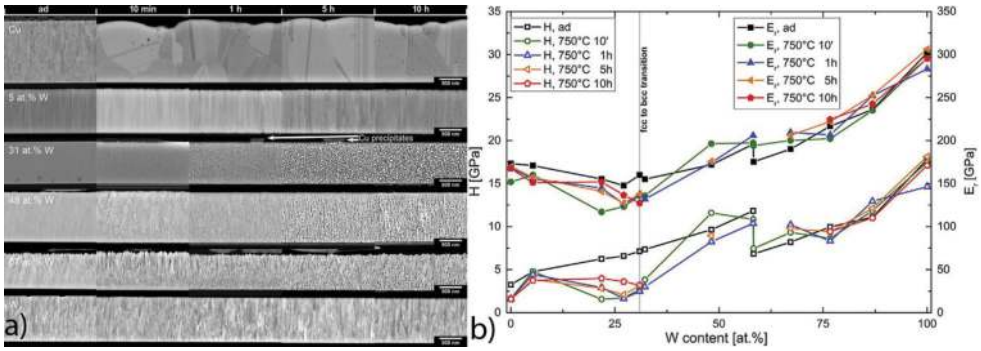

Figure 14. (a) Cross-sectional SEM images (BSE) of as-deposited and annealed Cu-W thin films (left). (b) Hardness and reduced Young's modulus as function of compositional fraction of W with standard deviation error bars for the as-deposited and annealed states (right). Figure is taken with permission from Ref. [101].

terms of several strengthening mechanisms. They concluded that the hardening of the Cu-Cr films is mainly caused by grain size refinement whereas the effects of solid solution hardening can be neglected. Nevertheless, they did not consider the contributions from the global effect of solute atoms on the matrix [83] and GB segregation [84] to the measured hardness.

Numerous atomistic simulations have demonstrated that GB segregation can remarkably stabilize the grains and enhance the strength/hardness of alloyed systems, such as Cu-Ta [15] and Cu-Nb [84]. Using molecular dynamics simulations with an angular-dependent interatomic potential, Frolov et al. [15] investigated the Ta doping effect on the barrier for grain coarsening and robust performance of NC Cu-6.5 at.% Ta alloys. It is found that Ta segregation at GBs notably increases structural stability and mechanical strength, compared with their siblings with a uniform distribution of the same amount of Ta. With increasing temperature, the Ta atoms agglomerate and segregate at GBs in the form of nanoclusters. These nanoclusters effectively pin GBs and thus prevent grain growth. Vo et al. [84] also revealed that alloying additions that lower GB energy were found to dramatically increase the yield strength of the alloy, with dilute Cu–Nb alloys approaching the theoretical strength of Cu. Their findings indicate the strength is not controlled by the grain size alone, but rather by a combination of both the molar fraction of GB atoms and the degree of GB relaxation, as captured via a new strengthening model for the NC materials. Based on the finding that strength increases with

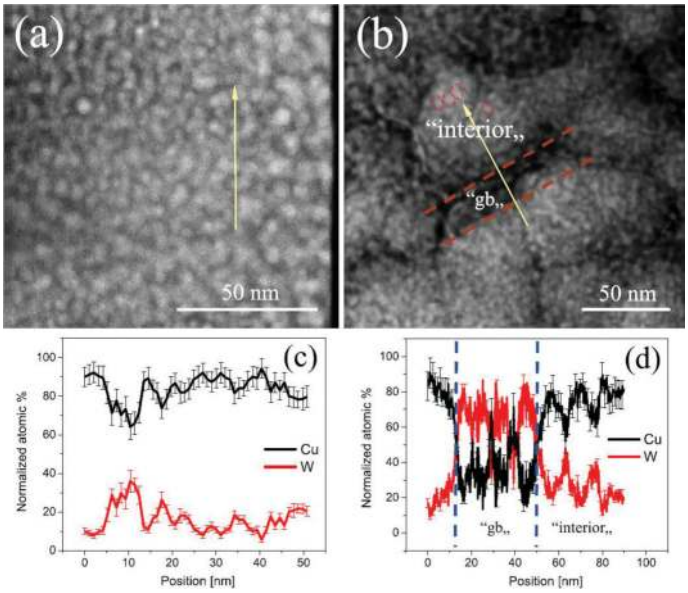

Figure 15. Cross-sectional (a) and planar-view (b) HAADF-TEM images of the annealed Cu(W)-14 thin film. The planar-view TEM image shows the prevailing columnar morphology with relatively broad grain (column) boundary regions between the columns. EDS analyses (c, d) performed by TEM reveal an inhomogeneous solute atom distribution indicating the nanoscale decomposition process. Figure is taken with permission from Ref. [104].

increasing atomic volume of the solute, they also predicted the possibility of achieving a theoretical strength in Cu by doping suitable solute atoms [84].

In parallel, Csiszár et al. [104] investigated the stability of NT Cu-W alloyed films during annealing in the range of 30–600°C, compared with their Ni-W and Ag-W NT siblings. A major, microstructural difference observed for all films upon annealing is the redistribution of the alloying element (W) content. In the case of Cu-14 at.% W, a significant redistribution of W was detected by TEM and EDS (see **Figure 15**), similar to the case of Ag-13 at.% W film but far different from that of Ni-12 at.% W film associated with a redistribution of the W atoms on an apparently very fine spatial scale. Their TEM analysis shows that an obviously nanoscale phase separation emerges throughout the Cu-14 at.% W film (see **Figure 15**). The size and the composition of the nanoinclusions at the GBs and in the grain (column) interiors are different, see **Figure 15(d)**. At the GBs, the average precipitates (rich in W) have dimensions of about 5–6 nm in diameter and in the grain interiors the precipitates (rich in Cu) are twice as large, see **Figure 15(d)**. Interestingly, the TBs are largely preserved in Ag-W and Ni-W films, whereas they completely disappear in Cu-W films. They attributed this unique phenomenon to an altered faulting energy, due to change in the amount of W segregated at TBs and to the evolution of nanosized precipitates [104]. This systematical, representative study of W-alloyed, heavily faulted NS thin films not only provides deep insights into understanding the atomic interactions in the binary alloyed films with high positive H_{mix} like Cu-W system, but also benefits us to tune their microstructural stability and mechanical properties in future.

5. Summary

The metallic thin films become essential structural materials in micro- and nanodevices and refining grain size into nanoscale indeed can notably increase their strength and strain-rate sensitivity, whereas they undergo the strength-ductility tradeoff on the one hand and suffer from unstable microstructure, i.e., grain growth, on the other. How to defect the conflict between strength and ductility and simultaneously retain highly stable microstructure is a grand challenge in the material community. The GB segregation engineering seems to open a promising avenue for the design of alloyed thin films with superior property combinations by tuning their multihierarchical structures utilizing alloying additions. The twinning-mediated grain growth is a novel and effective method to toughen the NS FCC metals and alloys with exceptionally high values of both strength and ductility. The effects of GB complexions on static and dynamic properties are far different in the alloyed thin films, and more works require to be performed in the future.

Acknowledgements

This work was supported by the National Natural Science Foundation of China (Grant Nos. 51621063, 51321003, 51571157, 51322104 and 51201123) and the 111 Project of China (B06025).

GL thanks the support from the National Science Find for Distinguished Yong Scholars. JYZ is grateful for Natural Science Basic Research Plan in Shaanxi Province of China (Program No. 2015JM5158) and China Postdoctoral Science Foundation (2016M590940) for part of financial support.

Author details

Jinyu Zhang*, Gang Liu* and Jun Sun*

*Address all correspondence to: jinyuzhang1002@mail.xjtu.edu.cn, lgsammer@mail.xjtu.edu.cn and junsun@mail.xjtu.edu.cn

State Key Laboratory for Mechanical Behavior of Materials, Xi'an Jiaotong University, Xi'an, PR China

References

[1] Arzt E. Size effects in materials due to microstructural and dimensional constraints: a comparative review. Acta Materialia. 1998;**46**(19):5611–5626.

[2] Meyers M.A., Mishra A., Benson D.J. Mechanical properties of nanocrystalline materials. Progress in Materials Science. 2006;**51**(4):427–556.

[3] Dao M., Lu L., Asaro R.J., De Hosson J.T.M., Ma E. Toward a quantitative understanding of mechanical behavior of nanocrystalline metals. Acta Materialia. 2007;**55**(12):4041–4065.

[4] Jin M., Minor A.M., Stach E.A., Morris Jr J.W. Direct observation of deformation-induced grain growth during the nanoindentation of ultrafine-grained Al at room temperature. Acta Materialia. 2004;**52**(18):5381–5387.

[5] Zhang K., Weertman J.R., Eastman J.A. Rapid stress-driven grain coarsening in nanocrystalline Cu at ambient and cryogenic temperatures. Applied Physics Letters. 2005;**87**:061921.

[6] Gianola D.S., Van Petegem S., Legros M., Brandstetter S., Van Swygenhoven H., Hemker K.J. Stress-assisted discontinuous grain growth and its effect on the deformation behavior of nanocrystalline aluminum thin films. Acta Materialia. 2006;**54**(8):2253–2263.

[7] Rupert T.J., Gianola D.S., Gan Y., Hemker K.J. Experimental observations of stress-driven grain boundary migration. Science. 2009;**326**(5960):1686–1690.

[8] Kirchheim R. Grain coarsening inhibited by solute segregation. Acta Materialia. 2002;**50**(2):413–419.

[9] Kirchheim R. Reducing grain boundary, dislocation line and vacancy formation energies by solute segregation. I. Theoretical background. Acta Materialia. 2007;**55**(15):5129–5138.

[10] Kirchheim R. Reducing grain boundary, dislocation line and vacancy formation energies by solute segregation: II. Experimental evidence and consequences. Acta Materialia. 2007;**55**(15):5139–5148.

[11] Trelewicz J.R., Schuh C.A. Grain boundary segregation and thermodynamically stable binary nanocrystalline alloys. Physical Review B. 2009;**79**(9):094112.

[12] Chookajorn T., Murdoch H.A., Schuh C.A. Design of stable nanocrystalline alloys. Science. 2012;**337**:951–954.

[13] Murdoch H.A., Schuh C.A. Estimation of grain boundary segregation enthalpy and its role in stable nanocrystalline alloy design. Journal of Materials Research. 2013;**28**(16):2154–2163.

[14] Millett P.C., Selvam R.P., Saxena A. Stabilizing nanocrystalline materials with dopants. Acta Materialia. 2007;**55**(7):2329–2336.

[15] Frolov F., Darling K.A., Kecskes L.J., Mishin Y. Stabilization and strengthening of nanocrystalline copper by alloying with tantalum. Acta Materialia. 2012;**60**(5):2158–2168.

[16] Smith D. Thin-film deposition: principles and practice. New York: McGraw Hill Professional; 1995.

[17] Geng H. Semiconductor manufacturing handbook. 1stst ed. Blacklick: McGraw-Hill Professional; 2005.

[18] Erb U., Aust K.T., Palumbo G. Electrodeposited nanocrystalline metals, alloys and composites. In: Koch C.C., editor. Nanostructured materials – processing, properties, and applications. 2nd ed. New York: William Andrew; 2007. pp. 235–292.

[19] Erb U. Electrodeposited nanocrystals: synthesis, properties and industrial applications. Nanostructured Materials. 1995;**6**(5–8):533–538.

[20] Guo N.N., Zhang J.Y., Cheng P.M., Liu G., Sun J. Room temperature creep behavior of free-standing Cu films with bimodal grain size distribution. Scripta Materialia. 2013;**68**(11):849–852.

[21] Lu L., Chen X., Huang X., Lu K. Revealing the maximum strength in nanotwinned copper. Science. 2009;**323**(5914):607–610.

[22] Lu L., Shen Y.F., Chen X., Qian L., Lu K. Ultrahigh strength and high electrical conductivity in copper. Science. 2004;**304**(5669):422–426.

[23] Niu R.M., Liu G., Wang C., Zhang G.J., Ding X.D., Sun J. Thickness dependent critical strain in submicron Cu films adherent to polymer substrate. Applied Physics Letters. 2007;**90**(16):161907.

[24] Sun X.J., Wang C., Zhang J., Liu G., Zhang G.J., Ding X.D., et al. Thickness dependent fatigue life at microcrack nucleation for metal thin films on flexible substrates. Journal of Physics D: Applied Physics. 2008;**41**:195404.

[25] Yamakov V., Wolf D., Phillpot S.R., Mukherjee A.K., Gleiter H. Deformation-mechanism map for nanocrystalline metals by molecular-dynamics simulation. Nature Materials. 2004;**3**:43–47 .

[26] Yamakov V., Wolf D., Phillpot S.R., Mukherjee A.K., Gleiter H. Dislocation processes in the deformation of nanocrystalline aluminium by molecular-dynamics simulation. Nature Materials. 2002;**1**:45–49.

[27] Van Swygenhoven H., Derlet P.M., Frøseth A.G. Nucleation and propagation of dislocations in nanocrystalline fcc metals. Acta Materialia. 2006;**54**(7):1975–1983.

[28] Budrovic Z., Van Swygenhoven H., Derlet P.M., Van Petegem S., Schmitt, B. Plastic deformation with reversible peak broadening in nanocrystalline nickel. Science. 2004;**304**:273–276.

[29] Oh S.H., Legros M., Kiener D., Gruber P., Dehm G. In situ TEM straining of single crystal Au films on polyimide: Change of deformation mechanisms at the nanoscale. Acta Materialia. 2007;**55**(16):5558–5571.

[30] Wu X.L., Zhu Y.T. Inverse grain-size effect on twinning in nanocrystalline Ni. Physical Review Letters. 2008;**101**:025503.

[31] Zhang J.Y., Liu G., Wang R.H., Li J., Ma E., Sun J. Double-inverse grain size dependence of deformation twinning in nanocrystalline Cu. Physical Review B. 2010;**81**(17):172104.

[32] Zhang J.Y., Zhang P., Wang R.H., Liu G., Zhang G.J., Sun J. Grain-size-dependent zero-strain mechanism for twinning in copper. Physical Review B. 2012;**86**(6):064110.

[33] Mompiou F., Caillard D., Legros M., Mughrabi H. In situ TEM observations of reverse dislocation motion upon unloading in tensile-deformed UFG aluminium. Acta Materialia. 2012;**60**(8):3402–3414.

[34] Hu J.J., Zhang J.Y., Jiang Z.H., Ding X.D., Zhang Y.S., Han S., et al. Plastic deformation behavior during unloading in compressive cyclic test of nanocrystalline copper. Materials Science and Engineering: A. 2016;**651**:999–1009.

[35] Asaro R.A., Suresh S. Mechanistic models for the activation volume and rate sensitivity in metals with nanocrystalline grains and nano-scale twins. Acta Materialia. 2005;**53**(12):3369–3382.

[36] Sedlmayr A., Bitzek E., Gianola D.S., Richter G., Mönig R., Kraft O. Existence of two twinning-mediated plastic deformation modes in Au nanowhiskers. Acta Materialia. 2012;**60**(9):3985–3993.

[37] Li J., Zhang J.Y., Jiang L., Zhang P., Wu K., Liu G., et al. Twinning/detwinning-mediated grain growth and mechanical properties of free-standing nanotwinned Ni foils: grain size and strain rate effects. Materials Science and Engineering: A. 2015;**628**:62–74.

[38] Schiøtz J., Jacobsen K. W. A maximum in the strength of nanocrystalline copper. Science. 2003;**301**(5638):1357–1359.

[39] Shan Z., Stach E., Wiezorek J., Knapp J., Follstaedt D., Mao S. Grain boundary-mediated plasticity in nanocrystalline nickel. Science. 2004;**305**(5684):654–657.

[40] Schiøtz J., Di Tolla F.D., Jacobsen K.W. Softening of nanocrystalline metals at very small grain sizes. Nature. 1998;**391**(6667):561–563.

[41] Carlton C.E., Ferreira P.J. What is behind the inverse Hall-Petch effect in nanocrystalline materials? Acta Materialia. 2007;**55**(11):3749–3756.

[42] Wang Y.M., Sansoz F., Lagrange T., Ott R.T., Marian J., Barbee Jr T.W., et al. Defective twin boundaries in nanotwinned metals. Nature Materials. 2013;**12**(8):697–702.

[43] Lu N., Du K., Lu L., Ye H.Q. Transition of dislocation nucleation induced by local stress concentration in nanotwinned copper. Nature Communications. 2015;**6**:7648.

[44] Li X.Y., Wei Y.J., Lu L., Lu K., Gao H.J. Dislocation nucleation governed softening and maximum strength in nano-twinned metals. Nature. 2010;**464**:877–880.

[45] Mohamed F.A. A dislocation model for the minimum grain size obtainable by milling. Acta Materialia. 2003;**51**(14):4107–4119.

[46] Edalati K., Horita Z. High-pressure torsion of pure metals: influence of atomic bond parameters and stacking fault energy on grain size and correlation with hardness. Acta Materialia. 2011;**59**(17):6831–6836.

[47] Li J., Zhang J.Y., Liu G., Sun J. New insight into the stable grain size of nanotwinned Ni in steady-state creep: effect of the ratio of effective-to-internal stress. International Journal of Plasticity. 2016;**85**:172–189.

[48] Luo X.M., Zhu X.F., Zhang G.P. Nanotwin-assisted grain growth in nanocrystalline gold films under cyclic loading. Nature Communications. 2014;**5**:3021.

[49] Kohama K., Ito K., Matsumoto T., Shirai Y., Murakami M. Role of cu film texture in grain growth correlated with twin boundary formation. Acta Materialia. 2012;**60**(2):588–595.

[50] Zhu Y.T., Wu X., Liao X., Narayan J., Kecskes L., Mathaudhu S. Dislocation–twin interactions in nanocrystalline fcc metals. Acta Materialia. 2011;**59**(2):812–821.

[51] Cao Y., Wang Y., An X., Liao X., Kawasaki M., Ringer S., et al. Grain boundary formation by remnant dislocations from the de-twinning of thin nano-twins. Scripta Materialia. 2015;**100**:98–101.

[52] Tao N.R., Lu K. Nanoscale structural refinement via deformation twinning in face-centered cubic metals. Scripta Materialia. 2009;**60**(12):1039–1043.

[53] Kraft O., Hommel M., Arzt E. X-ray diffraction as a tool to study the mechanical behaviour of thin films. Materials Science and Engineering: A. 2000;**288**(2):209–216.

[54] Yu D.Y.W., Spaepen F. The yield strength of thin copper films on kapton. Journal of Applied Physics. 2004;**95**(6):2991–2997.

[55] Zhang G.P., Sun K.H., Zhang B., Gong J., Sun C., Wang, Z.G. Tensile and fatigue strength of ultrathin copper films. Materials Science and Engineering: A. 2008;**483–484**:387–390.

[56] Gruber P.A., Böhm J., Onuseit F., Wanner A., Spolenak R., Arzt E. Size effects on yield strength and strain hardening for ultra-thin cu films with and without passivation: a study by synchrotron and bulge test techniques. Acta Materialia. 2008;**56**(10):2318–2335.

[57] Zhang J.Y., Zhang X., Liu G., Wang R.H., Zhang G.J., Sun J. Length scale dependent yield strength and fatigue behaviour of nanocrystalline Cu thin film. Materials Science and Engineering: A. 2011;**528**(25–26):7774–7780.

[58] Zhang J.Y., Zhang P., Wang R.H., Liu G., Zhang G.J., Sun J. Enhanced mechanical properties of columnar grained-nanotwinned Cu films on compliant substrate via multilayer scheme. Materials Science and Engineering: A. 2012;**554**:116–121.

[59] Wang Y., Chen M., Zhou F., Ma E. High tensile ductility in a nanostructured metal. Nature. 2002;**419**:912–915.

[60] Wang Y.M., Ott R.T., Hamza A.V., Besser M.F., Almer J., Kramer M.J. Achieving large uniform tensile ductility in nanocrystalline metals. Physical Review Letters. 2010;**105**(21):215502.

[61] Zhu T., Li J. Ultra-strength materials. Progress in Materials Science. 2010;**55**(7):710–757.

[62] Wei Q., Cheng S., Ramesh K.T., Ma E. Effect of nanocrystalline and ultrafine grain sizes on the strain rate sensitivity and activation volume: fcc versus bcc metals. Materials Science and Engineering: A. 2004;**381**(1–2):71–79.

[63] Chen J., Lu L., Lu K. Hardness and strain rate sensitivity of nanocrystalline Cu. Scripta Materialia. 2006;**54**(11):1913–1918.

[64] Schwaiger R., Moser B., Dao M., Chollacoop N., Suresh S. Some critical experiments on the strain-rate sensitivity of nanocrystalline nickel. Acta Materialia. 2003;**51**(17):5159–5172.

[65] Torre F.D., Spatig P., Schaublin R., Victoria M. Deformation behaviour and microstructure of nanocrystalline electrodeposited and high pressure torsioned nickel. Acta Materialia. 2005;**53**(8):2337–2349.

[66] Wang Y.M., Hamza A.V., Ma E. Temperature-dependent strain rate sensitivity and activation volume of nanocrystalline Ni. Acta Materialia. 2006;**54**(10):2715–2726.

[67] Pan D., Nieh T.G., Chen M.W. Strengthening and softening of nanocrystalline nickel during multistep nanoindentation. Applied Physics Letters. 2006;**88**(16):161922.

[68] Jennings A.T., Li J., Greer J.R. Emergence of strain-rate sensitivity in Cu nanopillars: transition from dislocation multiplication to dislocation nucleation. Acta Materialia. 2011;**59**(14):5627–5637.

[69] Zhang J.Y., Liang X.Q., Zhang P., Wu K., Liu G., Sun J. Emergence of external size effects in the bulk-scale polycrystal to small-scale single-crystal transition: a maximum in the strength and strain-rate sensitivity of multicrystalline Cu micropillars. Acta Materialia. 2014;**66**:302–316.

[70] Lu L., Zhu T., Shen Y., Dao M., Lu K., Suresh S. Stress relaxation and the structure size-dependence of plastic deformation in nanotwinned copper. Acta Materialia. 2009;**57**(17):5165–5173.

[71] Li J., Zhang J.Y., Zhang P., Wu K., Liu G., Sun J. Grain size effects on microstructural stability and creep behavior of nanotwinned Ni free-standing foils at room temperature. Philosophical Magazine. 2016;**96**(29):3016–3040

[72] Niu J.J., Zhang J.Y., Liu G., Zhang P., Lei S.Y., Zhang G.J., Sun J. Size-dependent deformation mechanisms and strain-rate sensitivity in nanostructured Cu/X (X = Cr, Zr) multilayer films. Acta Materialia. 2012;**60**(9):3677–3689.

[73] Zhang G.P., Volkert C.A., Schwaiger R., Wellner P., Arzt E., Kraft O. Length-scale-controlled fatigue mechanisms in thin copper films. Acta Materialia. 2006;**54**(11):3127–3139.

[74] Liu G., Zhang G.J., Jiang F., Ding X.D., Sun Y.J., Sun J., et al. Nanostructured high-strength molybdenum alloys with unprecedented tensile ductility. Nature Materials. 2013;**12**(4):344–350.

[75] Weissmüller J. Alloy effects in nanostructures. Nanostructured Materials. 1993;**3**(1–6):261–272.

[76] Seidman D.N. Subnanoscale studies of segregation at grain boundaries: simulations and experiments. Annual Review of Materials Research. 2002;**32**(1):235–269.

[77] Liu F., Kirchheim R. Nano-scale grain growth inhibited by reducing grain boundary energy through solute segregation. Journal of Crystal Growth. 2004;**264**(1–3):385–391.

[78] Raabe D., Herbig M., Sandlöbes S., Li Y., Tytko D., Kuzmina M., et al. Grain boundary segregation engineering in metallic alloys: a pathway to the design of interfaces. Current Opinion in Solid State and Materials Science. 2014;**18**(4):253–261.

[79] Lejček P., Zheng L., Hofmann S., Šob M. Applied thermodynamics: grain boundary segregation. Entropy. 2014;**16**(3):1462–1483.

[80] Saber M., Koch C.C., Scattergood R.O. Thermodynamic grain size stabilization models: an overview. Materials Research Letters. 2015;**3**(2):65–75.

[81] Peng H., Chen Y., Liu F. Effects of alloying on nanoscale grain growth in substitutional binary alloy system: thermodynamics and kinetics. Metallurgical & Materials Transactions A. 2015;**46**(11):5431–5443.

[82] Zhang P., Zhang J.Y., Li J., Liu G., Wu K., Wang Y.Q., Sun J. Microstructural evolution, mechanical properties and deformation mechanisms of nanocrystalline Cu thin films alloyed with Zr. Acta Materialia. 2014;**76**:221–237.

[83] Rupert T.J., Trenkle J.C., Schuh, C.A. Enhanced solid solution effects on the strength of nanocrystalline alloys. Acta Materialia. 2011;**59**(4):1619–1631.

[84] Vo N.Q., Schäfer J., Averback R.S., Albe K., Ashkenazy Y., Bellon P. Reaching theoretical strengths in nanocrystalline Cu by grain boundary doping. Scripta Materialia. 2011;**65**(8):660–663.

[85] Cahn J.W. The impurity-drag effect in grain boundary motion. Acta Metallurgica. 1962; **10**(9):789–798.

[86] Schwarze C., Kamachali R.D., Steinbach I. Phase-field study of zener drag and pinning of cylindrical particles in polycrystalline materials. Acta Materialia. 2016;**106**:59–65.

[87] Pan Z.L., Rupert T.J. Amorphous intergranular films as toughening structural features. Acta Materialia. 2015;**89**:205–214.

[88] Wang Y.M., Li J., Hamza A.V., Barbee Jr T.W. Ductile crystalline-amorphous nanolaminates. Proceedings of the National Academy of Sciences of the United States of America. 2007;**104**(27):11155–11160.

[89] Zhang J.Y., Liu G., Lei S., Niu J.J., Sun J. Transition from homogeneous-like to shear-band deformation in nanolayered crystalline Cu/amorphous Cu–Zr micropillars: intrinsic vs. extrinsic size effect. Acta Materialia. 2012;**60**(20):7183–7196.

[90] Wang Y.Q., Zhang J.Y., Liang X.Q., Wu K., Liu G., Sun J. Size- and constituent-dependent deformation mechanisms and strain rate sensitivity in nanolaminated crystalline Cu/amorphous Cu–Zr films. Acta Materialia. 2015;**95**:132–144.

[91] Schäfer J., Stukowski A., Albe K. Plastic deformation of nanocrystalline Pd–Au alloys: on the interplay of grain boundary solute segregation, fault energies and grain size. Acta Materialia. 2011;**59**(8):2957–2968.

[92] Zhang P., Zhang J.Y., Li J., Liu G., Wu K., Wang Y.Q., et al. Combined effect of texture and nanotwins on mechanical properties of the nanostructured Cu and Cu–Al films prepared by magnetron sputtering. Journal of Materials Science. 2015;**50**(4):1901–1907.

[93] Heckman N.M., Velasco L., Hodge A.M. Influence of twin thickness and grain size on the tensile behavior of fully nanotwinned CuAl alloys. Advanced Engineering Materials. 2016;**18**(6):918–922

[94] Brons J.G., Thompson G.B. Abnormalities associated with grain growth in solid solution Cu (Ni) thin films. Thin Solid Films. 2014;**558**:170–175.

[95] Millett P.C., Selvam R.P., Bansal S., Saxena A. Atomistic simulation of grain boundary energetics – effects of dopants. Acta Materialia. 2005;**53**(13):3671–3678.

[96] Millett P.C., Selvam R.P., Saxena A. Molecular dynamics simulations of grain size stabilization in nanocrystalline materials by addition of dopants. Acta Materialia. 2006;**54**(2):297–303.

[97] Detor A.J., Schuh C.A. Grain boundary segregation, chemical ordering and stability of nanocrystalline alloys: atomistic computer simulations in the Ni–W system. Acta Materialia. 2007;**55**(12):4221–4232.

[98] Chookajorn T., Schuh C.A. Thermodynamics of stable nanocrystalline alloys: a Monte Carlo analysis. Physical Review B. 2014;**89**(6):064102.

[99] Bedorf D., Mayr S.G. Grain boundary doping of Cu thin films with Bi: a route to create smooth and stable nanocrystalline surfaces. Scripta Materialia. 2007;**57**(9):853–856.

[100] Keast V.J., La Fontaine A., du Plessis J. Variability in the segregation of bismuth between grain boundaries in copper. Acta Materialia. 2007;**55**(15):5149–5155.

[101] Vüllers F.T.N., Spolenak R. From solid solutions to fully phase separated interpenetrating networks in sputter deposited "immiscible" W-Cu thin films. Acta Materialia. 2015;**99**:213–227.

[102] Harzer T.P., Djaziri S., Raghavan R., Dehm G. Nanostructure and mechanical behavior of metastable Cu–Cr thin films grown by molecular beam epitaxy. Acta Materialia. 2015;**83**:318–332.

[103] Müller C.M., Sologubenko A.S., Gerstl S.S.A., Spolenak R. On spinodal decomposition in cu–34at.% ta thin films – an atom probe tomography and transmission electron microscopy study. Acta Materialia. 2015;**89**:181–192.

[104] Csiszár G., Kurz S.J.B., Mittemeijer E.J. Stability of nanosized alloy thin films: faulting and phase separation in metastable Ni/Cu/Ag-W films. Acta Materialia. 2016;**110**:324–340.